PCCP

PAPER

View Article Online
View Journal | View Issue

Cite this: *Phys. Chem. Chem. Phys.*, 2015, **17**, 21364

Received 11th February 2015,
Accepted 5th March 2015

DOI: 10.1039/c5cp00884k

www.rsc.org/pccp

The adsorption of thiophenol on gold – a spectroelectrochemical study

Rudolf Holze

The adsorbate formed by adsorption of thiophenol on a polycrystalline gold electrode and brought into contact with aqueous solutions of 1 M $HClO_4$ and 0.1 M $KClO_4$ has been studied using cyclic voltammetry and surface-enhanced Raman spectroscopy. A strong adsorption is deduced from observations made using cyclic voltammetry. From the SER spectra, interactions of thiophenol with the gold surface *via* a gold–sulfur bond with the aromatic ring pointing away from the surface is concluded for both electrolyte solutions.

Introduction

Substantial interest has been devoted to studies of self-assembled monolayers (SAMs) formed in particular of sulfur-containing (*i.e.* mostly –SH– and less frequently –SR–substituted) organic molecules on gold surfaces.[1–3] Unfortunately the term SAM has gained a huge popularity although sometimes not matching the actual properties of the layers, in particular their degree of ''organization'', *i.e.* periodicity. As reported elsewhere[4] the initially formed adsorbates are not necessarily well-organized and may reorganize on the surface into some better organized forms,[5] but the highly organized arrangements frequently shown are not always obtained. Because SAMs on gold electrodes hold particular potential regarding the modification of the surface properties, patterning *etc.* published reports on electrochemical, spectroelectrochemical and surface-analytical studies are numerous. Somewhat surprisingly the most simple molecule thiophenol† TP has barely attracted attention beyond particular applications briefly reviewed below. Its adsorption on a mercury electrode has been studied,[6] the Gibbs energy of adsorption $\Delta G_{ad} = -25.55$ kJ mol^{-1} implies physisorption only. The respective value observed with a platinum electrode $\Delta G_{ad} = -41.0$ kJ mol^{-1} (ref. 7) suggests a moderately stronger interaction in the range of chemisorption. No respective values for gold have been reported presumably because of the very strong gold–sulfur interaction making most methods employed in adsorption studies and based on adsorption/desorption equilibria unsuitable;[8] the same applies apparently to silver. Data obtained for the adsorption of a number of other thio-compounds, in particular aliphatic ones, in the range $\Delta G_{ad} = -80$–100 kJ mol^{-1} again imply very strong chemisorption.[8] Various estimates and theoretical calculations reviewed by Ulman have resulted in a value of 167.15 kJ mol^{-1} for the Au–S-bond.[9] In order to close the gap in structural information – the thermodynamic one will hardly be closed at all with electrochemical methods – and to extend the initial data reported in an exploratory study by Szafranski *et al.*[10] we have studied the adsorption of thiophenol on a polycrystalline gold electrode using cyclic voltammetry (CV) and surface-enhanced Raman spectroscopy (SERS).[11]

Carron and Hurley have used SERS and TP adsorbed on copper, silver and gold surfaces to determine the azimuthal angle at the sulfur atom.[12] A study of TP adsorbed on gold nanoparticles has been reported by Li *et al.*[13] wherein theoretical data pertaining to the various states of the adsorbate have been obtained using DFT and compared with experimental data. The forms of species considered in theory were as follows.

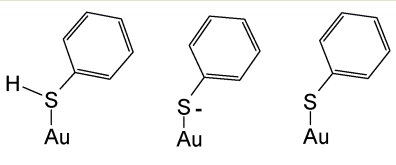

1 2 3

Scheme 1

Gold was implemented as a single atom instead of a cluster or an even larger aggregate resembling a solid. Adsorption as a thiophenylate (or simply thiolate) (**3**) was deduced from a comparison of calculated and experimentally observed band positions. A band observed at 275 cm^{-1} was assigned to the Au–S stretching mode. The calculated value of 334 cm^{-1} deviates strongly, presumably indicating the limited viability of representing a metal surface (even that of a nanoparticle) by

Technische Universität Chemnitz, Institut für Chemie, AG Elektrochemie, 09107 Chemnitz, Germany. E-mail: rudolf.holze@chemie.tu-chemnitz.de

† Popular synonyms are: phenylmercaptan, benzenethiol.

a single metal atom. It should be noted that generally adsorption of thiols is assumed to proceed *via* release of a hydrogen atom according to

$$R\text{–}S\text{–}H + Au_x \rightarrow RS^{(-)}Au^{(+)}Au_{x-1} + 1/2H_2$$

Accordingly the distinction between **2** and **3** in the preceding scheme is applicable only for a discrete species as assumed for the DFT calculations, a negatively charged adsorbate $RS^{(-)}$ with a metal surface being expected only at sufficiently negative electrode potentials. Both theoretical and experimental evidence supporting this assumption and the distinction between RS and $RS^{(-)}$ appears to be missing so far.

Further studies of adsorbed TP are available. In a study aiming at the separation of electromagnetic and chemical enhancement, Saikin *et al.*[14] assigned a band at 415 cm^{-1} as being admixed with the Au–S stretching mode. Wu *et al.*[15] prepared differently shaped gold particles subsequently studied with SER supplemented with DFT-calculations wherein the gold surface was mimicked by 9–16 atoms. Some of the displayed spectra (without band assignment) showed a band around 250 cm^{-1} possibly associated with a gold–sulfur mode. Form **3** was deduced from DFT-calculations, also assuming the interaction of a single gold atom with TP by Xu *et al.*[16] Surprisingly no band could be attributed to the ν_{Au-S} mode. Nara *et al.*[17] used an assembly of gold atoms arranged according to the Au(111) surface. The molecule was calculated with a tilting angle of 61° with respect to the surface normal.

In most studies involving the use of TP the molecule is used as a marker or reporter molecule or simply as a probe to determine the suitability of a substrate for surface enhancement or to estimate an enhancement factor (for examples, see ref. 18–23, for recent overviews see ref. 24, on theory see ref. 25 and 26). Joo adsorbed TP and benzyl mercaptan on gold nanoparticles.[27] Adsorption of the latter compound proceeded faster; at high bulk concentration of the adsorbate the obtained SER spectra were almost identical. At lower bulk concentration differences were observed, but neither a low-wavenumber band indicative of Au–S-interaction was observed nor band assignment and interpretation in terms of the adsorbate geometry were attempted. The suitability of gold colloids for SERS was examined by Xu *et al.*[28] using TP as a test molecule. TP induced the aggregation of the nanoparticles. Aggregation of gold nanoframes usually assumed to give enhanced scattering caused by the enhanced plasmonic field between the particles was found to actually reduce the enhancement of SERS by TP by Mahmoud and El-Sayed.[29] The observations could be described and explained using a discrete dipole approximation. The observed and assigned bands showed different increases of enhancement as a function of the number of involved nanoframes and interparticle separation. The type of TP–gold interaction was not discussed. Gold nanoparticles arranged as dimers with hot spots at their point of contact were prepared and tested by Alexander *et al.*[30] using TP as a test case. Only spectra in the fingerprint region were reported without band assignment, and a pronounced relationship between the plane of polarization of the illuminating light and the dimer axis was found. TP was employed as a test molecule to determine enhancement factors by Taylor *et al.*[31] and to determine the actual surface areas by Buividas *et al.*[32]

Ren *et al.*[33] applied tip-enhanced Raman spectroscopy to TP adsorbed on Au(110). The spectra were hardly different from those of plain TP. No metal–sulfur mode was found, no molecular orientation was deduced. For further studies surface selection rules not specified were invoked. Employing the vibrational Stark effect Marr and Schultz have imaged electric fields in both SERS and TERS using TP as a probe.[34] Fan *et al.*[35] used TP as a test molecule for estimation of the damping effect of a SiO_2-shell on a gold nanoparticle. The electromagnetic enhancement was found to decrease with growing shell thickness. Wang *et al.*[36] reported on Au–Ag-alloy nanoparticles with different compositions. TP was used as a probe molecule in subsequent studies using SERS. SER intensities increased with growing gold content at a laser wavelength of λ_0 = 1064 nm. Taking into account particle size and particle aggregation the higher gold content was related to the effect of surface plasmon resonance enhancement. SERS-active gold–silver nanofibers were prepared by electrospinning.[37] The actually observed enhancement for TP (among other molecules) depended on the gold content. Ling *et al.*[38] prepared silver nanowires coated with gold. The spectra reported for the fingerprint region suggest the suitability of the nanowires for SERS; no band assignments or vibrational band of a gold–sulfur mode were provided. Gold-coated silver particles prepared for an immunoassay were prepared by Cui *et al.*[39] A pronounced dependency of the SERS-intensity on the metallic composition was found, and the intensity was generally stronger by a factor of ten when compared with silver nanoparticles. Monodisperse gold octahedra were prepared by Chang *et al.*[40] The surface plasmon resonance was found to increase with the particle size. Using TP as a test molecule, the suitability of the substrate for SERS was examined. The maximum enhancement was found at a particle size of 90 nm, and no signal at all was found at ~120 nm. Substrate effects of gold nanospheres and nanocubes have been reported by Mahmoud[41] and Mahmoud and El-Sayed[42] without information regarding the adsorbate structure. Bhuvana *et al.*[43] prepared carbon-assisted electroless gold as SERS substrate and observed an enhancement factor of 10^6–10^7 for TP adsorbed on this substrate. Slightly smaller enhancement factors were observed by Kim *et al.*[44] for patterned gold nanoparticle films with adsorbed TP. Li *et al.*[45] and Ge *et al.*[46] used TP as a reporter molecule on gold colloids subsequently employed in an immunoassay.

Tao *et al.*[47] have studied adsorbates of TP, benzyl mercaptan, biphenylthiol and 4-biphenylmethanethiol without and with alkoxy-substituents in the *para*-position on gold electrodes obtained by evaporation of gold on mica (see Scheme 2). The results of cyclic voltammetry, ellipsometry, scanning tunneling microscopy and infrared spectroscopy imply that for all benzyl mercaptans and 4-biphenylmethanethiols closely packed and ordered monolayers are formed. TP and biphenylthiols yield lower surface coverages. With longer *p*-alkoxy-chains increasing intermolecular interaction and closer packing are found. These subtle differences in behavior were attributed to the bond angle situation at the thiolate head group being in an interplay with

intermolecular interactions. Theoretical calculations assuming both sp^3- and sp-hybridization with respective adsorbate geometries have been reported;[48,49] unfortunately experimental evidence (in particular vibrational spectra) supporting the suggested sp-hybridization is lacking so far.

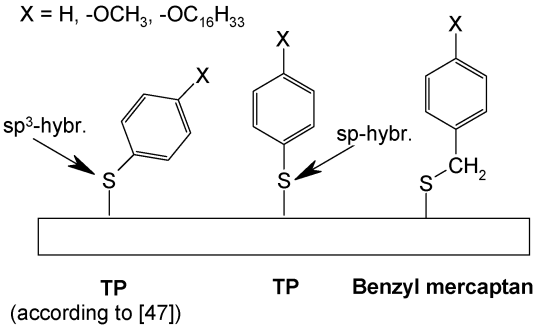

Scheme 2

Formation of poorly defined SAMs from TP was also deduced from contact angle measurements and ellipsometry by Sabatani *et al.*[50]

Several publications dealing with substituted TP (namely 4-nitrothiophenol, 4-amino-thiophenol[51] *etc.*) are available, mostly these molecules serve just as probes like TP, metal–sulfur vibrations are not mentioned. Dithiols, *i.e.* molecules with two –SH-units, show particularly poor organization.[4]

Somewhat surprisingly for TP and substituted TPs adsorbed on silver a corresponding silver–sulfur vibration was repeatedly not observed.[52–55] Nevertheless, molecular adsorbate orientations ranging from flat[54] to perpendicular[55] were suggested based on the dominance of an in-plane mode indicative of perpendicular orientation.[55–57] Only Joo *et al.*[58] have observed a band as a shoulder at 237 cm^{-1} assigned to the $\nu_{Ag–S}$; however, the authors concluded somewhat reluctantly a face-on adsorption on the surface of the silver sol particles.

Given this large body of both experimental and theoretical evidence the present study attempts to close an apparent gap: the lack of a structural model of TP adsorbed on a polycrystalline gold surface in contact with an electrolyte solution. Based on results of electrochemical experiments (cyclic voltammetry CV) and SERS the mode of adsorbate–surface interaction, the orientation of the adsorbed molecule with respect to the surface and its chemical state taking into account solution pH should be deduced.

Experimental

CVs were recorded using gold sheet working electrodes using aqueous solutions of 1 M $HClO_4$ (Acros, p.A.) and 0.1 M $KClO_4$ (Merck, p.A., pH = 4.90, unbuffered) as supporting electrolytes and a custom-built potentiostat interfaced with a standard PC *via* an ADDA-converter card operated using custom developed software. A relative hydrogen reference electrode[59,60] was used in the experiments with the acidic electrolyte solution, with the solution of 0.1 M $KClO_4$ a mercurous sulfate electrode (E_{MSE} = 0.375 V *vs.* a saturated calomel electrode SCE and 1.252 V *vs.* RHE in this electrolyte solution) was employed in order to avoid contamination of the electrolyte solution with specifically adsorbing chloride ions. A gold sheet was used as the counter electrode in an H-cell with compartments separated by glass frits.

SER spectra were recorded on an ISA T64000 spectrometer connected to a Spectraview 2D CCD detection system using λ_0 = 647.1 nm excitation laser light provided by a Coherent Innova 70 Series ion laser, the laser power was measured at the laser head with a Coherent 200 power meter. Normal Raman spectra of liquid thiophenol were recorded for comparison on a Mono-Vista CRS High Resolution spectrometer at λ_0 = 473 nm with exciting laser light provided by a Cobolt solid state laser at approx. 8 mW laser power at the sample. Infrared spectra were acquired on a BioRad FTS40 instrument at 2 cm^{-1} resolution with 32 scans and baseline-correction.

Roughening of the gold electrode (Schiefer, Hamburg, polycrystalline 99.99%, polished down to 0.3 μm Al_2O_3 to ascertain a defined clean surface state) employed to confer SERS activity was performed in a separate cell with an aqueous solution of 0.1 M KCl by cycling the electrode potential between E_{SCE} = −0.8 V and E_{SCE} = 1.65 V for about 10 minutes.[61]

Electrolyte solutions were prepared from 18 MOhm water (Seralpur Pro 90 c), thiophenol (Merck, z.S., used as received), perchloric acid (Acros, p.A.), and $KClO_4$ (Merck, Suprapur). All solutions were freshly prepared, purged with nitrogen (99.999%), and all experiments were performed at room temperature (20 °C).

Adsorption of thiophenol on the gold electrodes was performed by exposing the electrodes for 5 min[31] to 1 hour[62] to its solution (5 and 1 mM) in absolute ethanol (VWR, AnalaR, min. 99.8%) without any electrode potential control.

Results and discussion

Cyclic voltammograms recorded in an aqueous 1 M $HClO_4$ electrolyte solution with a gold electrode without and with preadsorbed thiophenol (t_{ad} = 5 min if not stated otherwise) starting at the negative potential limit are displayed in Fig. 1. In the positive going scan a substantial change in the current wave associated with the formation of the gold hydroxide/oxide layer is found. The cathodic reduction peak associated with the reductive conversion of the gold oxide/hydroxide surface layer is somewhat diminished. Thus this layer has been formed to a smaller extent. Consequently a substantial portion of the anodic charge must have been consumed in oxidation or at least oxidative desorption of the adsorbed thiolate. No attempt has been made to estimate the amount of coverage as applied elsewhere.[63] The duration of the adsorption (ranging from 5 to 60 min according to ref. 31 and 62) did not show qualitatively different results. The estimated amount of coverage deduced from the anodic charge was only slightly larger with a longer adsorption time as evidenced in the inset of Fig. 1. Consequently, all experiments were performed with the shorter adsorption time of 5 min.

CVs recorded in an aqueous 1 M $HClO_4$ electrolyte solution with a gold electrode without and with preadsorbed thiophenol (t_{ad} = 5 min) from the spontaneously established rest potential

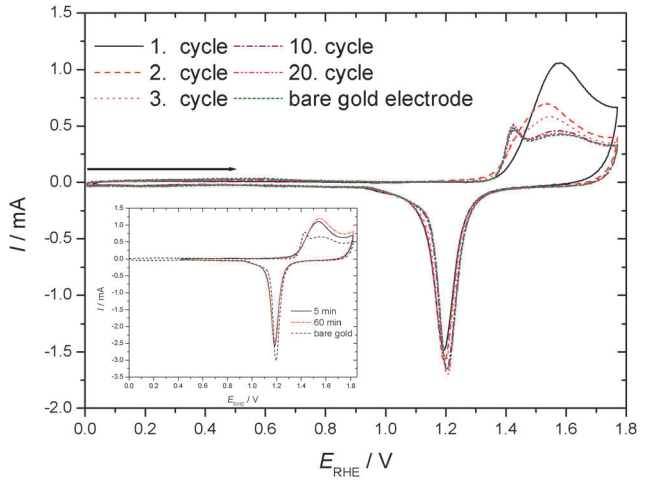

Fig. 1 Cyclic voltammograms of a gold sheet electrode without/with adsorbed TP in an aqueous solution of 1 M $HClO_4$ (full electrode potential cycles); dE/dt = 0.1 V s^{-1}, room temperature, nitrogen purged. Inset: effect of adsorption time.

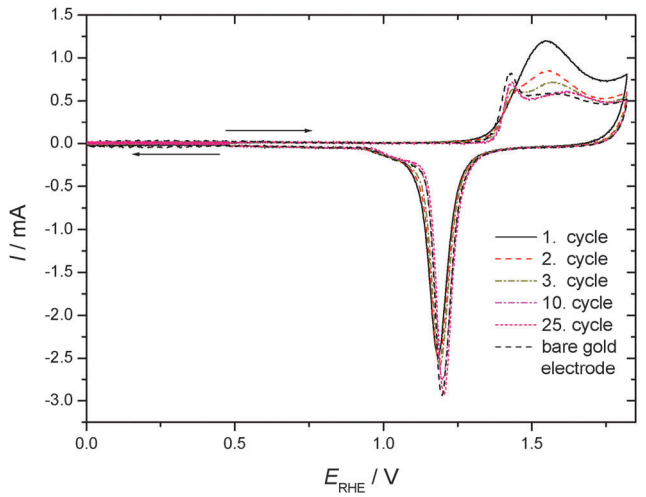

Fig. 2 Cyclic voltammograms of a gold sheet electrode without/with adsorbed TP in a solution of 1 M $HClO_4$ (partial cycles starting at spontaneous established rest potential, arrows indicate direction of scan with starting point of arrow indicating initial electrode potential); dE/dt = 0.1 V s^{-1}, room temperature, nitrogen purged.

towards anodic and cathodic directions are displayed in Fig. 2. This procedure does not risk electrode-potential induced changes, in particular desorption, caused by the initial potential step proceeding in the potential–time procedure applied for Fig. 1 where the electrode potential is switched from the rest potential established spontaneously at open circuit to the starting potential at the negative limit of the potential window where the first scan is initiated. No evidence of cathodic desorption or adsorbate reduction as reported elsewhere with *e.g.* 4-mercaptopyridine[64,65] is found in the negative going scan. In the positive going scan, again, a substantial change in the current wave associated with the formation of the gold hydroxide/oxide layer is found. Differences between the current response of the covered and the uncovered electrodes are similar to those observed with the different potential–time regime applied in the previous experiment (see Fig. 1). After about ten electrode potential cycles reaching into the oxygen evolution region the CV of a pristine, uncoated gold electrode is observed. Assuming that strength of interaction – in the remaining absence of precise thermodynamic data – can be related qualitatively to the number of electrode potential scans necessary to remove an adsorbate; this observation agrees closely with results obtained with *e.g.* 4-mercaptobenzonitrile.[66]

CVs recorded using TP adsorbed on a polycrystalline gold electrode subsequently exposed to an aqueous electrolyte solution of 0.1 M $KClO_4$ are shown in Fig. 3 for positive and negative going potential scans always starting at the spontaneously established rest potential. In comparison to the results obtained with an acidic electrolyte solution of well-defined pH-value a significantly different picture emerges. Oxidation of the gold electrode surface is strongly inhibited at less positive electrode potentials, but the anodic current finally observed at more positive potentials is more than double the value recorded with the supporting electrolyte solution. The associated reduction feature in the return scan usually assigned to a less strongly bound surface oxide, which is thus more easily reduced, is the same as that observed with the blank electrolyte solution, whereas the second reduction peak (at lower electrode potential) is almost absent. Accordingly the anodic current must be associated with formation of the less strongly bound surface oxide, and some charge (when taking the anodic charge as a measure) is consumed by an oxidative process involving TP without the formation of a strongly bound surface oxide.

SER spectra of TP preadsorbed on a roughened gold electrode in contact with an aqueous solution of 1 M $HClO_4$ are displayed in Fig. 5, as the reference vibrational spectra of TP are shown in Fig. 4. Assignment of bands as listed in Table 1 is based on literature data.[58,67–72] Interpretation of SER spectra aiming at elucidation of structural information ranging in the present case from the mode of interaction between TP and the gold surface to

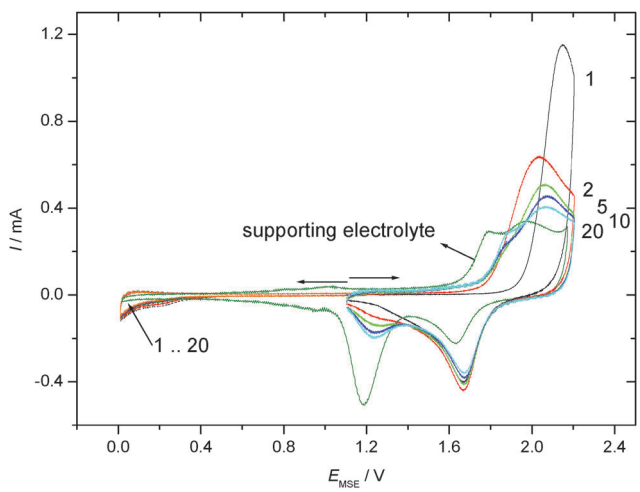

Fig. 3 Cyclic voltammograms of a gold sheet electrode without/with adsorbed TP in a solution of 0.1 M $KClO_4$ (full cycle, arrows indicate direction of scan with starting point of arrow indicating initial electrode potential); dE/dt = 0.1 V s^{-1}, room temperature, nitrogen purged.

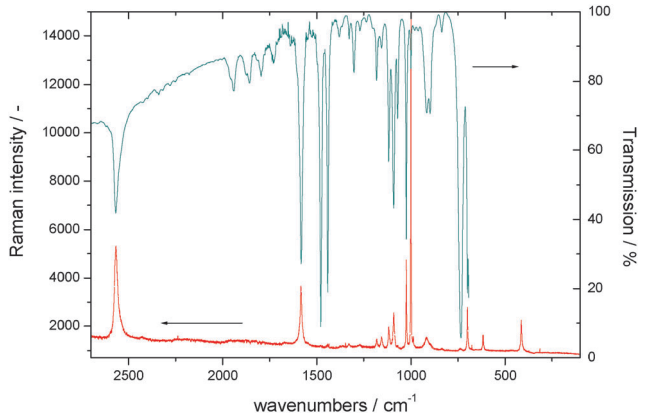

Fig. 4 Normal Raman and infrared spectra of thiophenol.

possible intermolecular interactions up to SAM-formation is based on (1) identification and assignment of bands not observed with the bulk molecule, changes in (2) band position and (3) intensity, for an introductory overview see ref. 73. The spectra show a band around 265 cm^{-1}, which does not appear for liquid thiophenol (Fig. 4),[70] becoming more pronounced and shifting towards lower wavenumbers with more positive electrode potentials. The shift implies a weaker bond at more positive electrode potentials. This in turn would not support adsorption of TP as a negatively charged species (see **2** in Scheme 1) but instead as an intact molecule R–S–H (showing a substantially weaker Au–S bond energy according to Li *et al.*[13]) or as thiolate C_6H_5S– as also proposed by Li *et al.*[13] Confusion with the C–S in-plane bending mode observed by Li *et al.*[13] at

Table 1 Spectral data of thiophenol and thiophenol adsorbed on a gold electrode at various electrode potentials from an aqueous solution of 1 M $HClO_4$, all assignments based on literature data[58,67–72]

					1 M $HClO_4$ (Fig. 5)			
Mode	#	Sym. C_{2v}^{γ} [a]	Infrared	NRS, Fig. 4	E_{RHE} = 0.2 V	E_{RHE} = 0.6 V	E_{RHE} = 0.8 V	E_{RHE} = 1 V
—	—	—	—	—	—	187	188	—
ν_{Au-S}	—	—	—	—	265	266	267	253
—	—	—	—	314	—	—	—	—
ν_{CH}	7a	a_1 ip	—	413 (412;413;412)[b]	416	420	419	419
ν_{ring}	16b oop	b_1 oop	—	— (464;461;462)	474	475	475	473
ν_{ring}	6b	b_2 ip	—	617 (617;617;615)	—	—	—	—
ν_{ring}	6a	a_1 ip	698	698 (698;698;697)	693	694	695	693
γ_{CH}	11 oop	b_1 oop	734	736 (736;734;737)	—	—	—	—
γ_{CH}	10a oop	a_1 oop	835	834 (834;836;836)	820	822	822	823
ν_{C-S-H}	—	—	916	916 (914;920;914)	933	933	933	933
γ_{CH}	5 oop	b_1 oop	—	988 (991;991;991)	—	—	—	—
ν_{ring}	12	a_1 ip	1000	1000 (1002;1000;1000)	998	999	999	999
δ_{CH}	18a	a_1 ip	1025	1024 (1026;1025;1024)	1022	1023	1023	1023
δ_{CH}	18b	b_2 ip	1071	(—;—;1070)	1073	1073	1073	1071
ν_{ring}	1	a_1 ip	1091	1091 (1091;1097;1092)				
Comb. mode	—	—	1118	1118 (—;—;1116)	1115	—	—	—
δ_{CH}	9b	b_2 ip	1156	1157 (1159;1154;1157)	1143	1144	1144	1142
δ_{CH}	9a	a_1 ip	1181	1181 (1182;1180;1180)	—	—	—	—
δ_{CH}	19b	b_2 ip	1441	—	—	—	—	—
δ_{CH}	19a	a_1 ip	1478	— (—;—;1481)	1472	1472	1473	1474
ν_{ring}	8a	a_1 ip	1582	1584 (1582;1582;1581)	1574	1574	1575	1571
—	—	—	—	—	—	—	1729	1729
ν_{S-H}	—	—	2569	2567 (2575;2566;2566)	—	—	—	—

δ = in-plane deformation, γ = out-of-plane deformation, ν = stretching, ν_s = symmetric stretching. β_{as} = rocking, ν_s = wagging, β_s = scissoring, # = Wilson mode number, all modes in-plane if not stated otherwise oop: out-of-plane. [a] Sometimes this is approximated as C_{2v} (*e.g.* in ref. 68). [b] Numbers in bracket refer to the assignments bei Varsanyi[69] (first value), Kohlrausch[67] (second value), and Scott *et al.*[68] (third value); #: Wilson mode number.

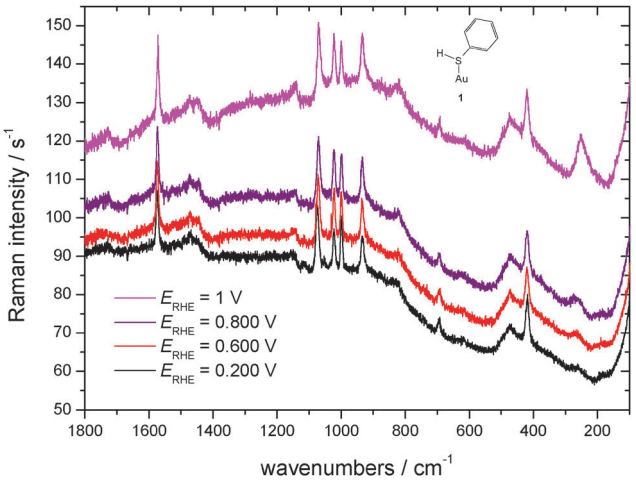

Fig. 5 SER-spectra of TP adsorbed on a polycrystalline gold electrode, aqueous solution of 1 M $HClO_4$, room temperature, nitrogen purged, for experimental conditions see text.

274 cm^{-1} with liquid TP but not seen here (see Fig. 4) is only theoretically possible, the extreme enhancement needed to support such assignment with the concomitant absence of a gold–sulfur mode makes it very unlikely. Distinction between the two options **1** and **3** (Scheme 1) is possible based on the intensity patterns and band positions reported by Li *et al.*[13] In the present case adsorption as intact TP can be deduced when taking into account the pronounced band at 933 cm^{-1} assigned to the C–S–H bending mode. The presence of a hydrogen atom at the sulfur atom will presumably have only a small steric effect pushing the aromatic ring closer to the metal surface and possibly diminishing surface enhancement of in-plane modes. This argument will thus hardly help to explain the lower overall SERS intensity.

For comparison SER spectra of related adsorbates interacting *via* the sulfur atom with the gold surface can be used. Several studies of thiol compounds adsorbed on gold surfaces by various authors have been reported,[10,12,74,75] for a brief overview see also ref. 65. Joo *et al.*[75] found a band at 227 cm^{-1} with benzyl phenyl sulfide adsorbed on a gold sol and assigned it to the Au–S stretching mode. Kang *et al.* assigned a band found for cyclohexyl isothiocyanate adsorbed at gold surfaces at 251 and 261 cm^{-1} (surprisingly depending on the adsorbate concentration in the deposition solution) to the Au–S stretching mode.[76] A band at 264 cm^{-1} was assigned by Bron and Holze[64,65] to the Au–S stretching of 4-mercaptopyridine adsorbed on a gold substrate. With the isomeric 2-mercaptopyridine this band was found at 235 cm^{-1}.[63] In a SERS study of adsorbed benzenethiol on gold a mode at 275 cm^{-1} not visible in the displayed spectra was assigned to the Au–S stretching.[12] Szafranski *et al.*[10] noticed a band at 270 cm^{-1} which was tentatively assigned either to the ring vibration mode ν_{15} or a gold–sulfur mode. Mode ν_{15} was neither observed in spectra of neat TP by Szafranski *et al.* nor by us (see Fig. 4); elsewhere, this band has been classified as weak.[69] Thus the band 265 cm^{-1} can be indeed assigned to the gold–sulfur mode implying an adsorbate orientation with the benzene ring pointing away from the electrode surface on the surface. Comparison of band intensities may provide evidence regarding molecular orientation. Although surface selection rules of the clear-cut type effective for infrared reflection spectroscopy as deduced by Greenler[77] are not available for SERS more complex ones have been deduced (see *e.g.* see ref. 78–82). As concluded elsewhere based on ample evidence particularly from comparative studies employing other tools of surface science vibrational modes perpendicular to the surface are particularly intense.[83,84] Assuming in slight simplification C_{2v} symmetry of TP the vibrational modes can be classified into in-plane a_1 and b_2 modes and out-of-plane a_2 and b_1 modes with all modes being Raman-active. Interaction with the surface may further reduce symmetry and – at least generally speaking – cause further Raman-silent modes to become active. As collected in Table 1 almost all observed bands are of the in-plane type. Thus it can be concluded, that TP is oriented with the aromatic ring pointing away from the electrode surface. A distinction between the suggested sp- or sp^3-hybridization and the corresponding bond angles is not possible with the evidence reported here and in the absence of vibrational spectroscopic evidence of sp-hybridization.

In Fig. 6 SER spectra of TP adsorbed on a polycrystalline gold electrode in contact with an aqueous electrolyte solution of 0.1 M $KClO_4$ are shown, band positions and assignments are collected in Table 2. A prominent change of relative intensity concerns the band at 933 cm^{-1} assigned to the C–S–H bending mode. Its relative weakness implies a relatively smaller amount of adsorbed R–S–H; accordingly R–S–dominates. The band assigned to the Au–S stretching mode is relatively weaker, its position shifts with positively going electrode potential to higher wavenumbers. Assuming thiolate as the adsorbed species the interaction (*i.e.* bond) will become stronger simply because of electrostatics (for other strongly adsorbed species see *e.g.* ref. 61).

No further significant changes in band positions and relative intensities are observed for both electrolyte solutions. This is in agreement both with the almost covalent attachment of the molecule *via* the sulfur atom and an orientation of the molecule away from the surface with less exposure to the electric field in the electrochemical double layer possibly yielding band shifts.

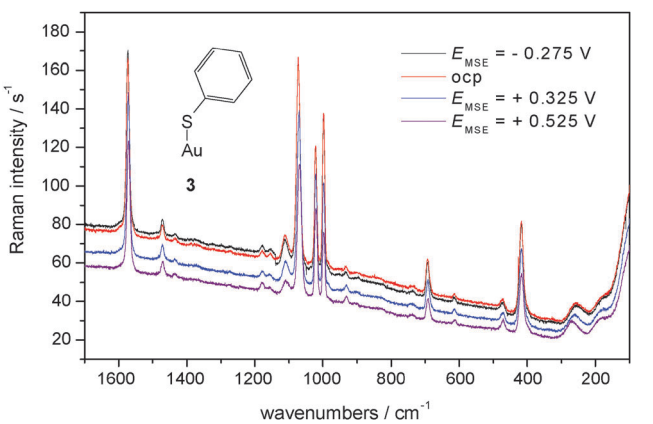

Fig. 6 SER-spectra of TP adsorbed on a polycrystalline gold electrode, aqueous solution of 0.1 M $KClO_4$, room temperature, nitrogen purged, for experimental conditions see text.

Table 2 Spectral data of thiophenol and thiophenol adsorbed on a gold electrode at various electrode potentials from an aqueous solution of 0.1 M $KClO_4$, all assignments based on literature data[58,67–72]

					0.1 M $KClO_4$ (Fig. 6)			
Mode	#	Sym. C_{2v}^{y}	Infrared	NRS, Fig. 4	E_{MSE} = 0.275 V	ocp	E_{MSE} = 0.325 V	E_{MSE} = 0.525 V
—	—	—	—	—	176	172	178	177
ν_{Au-S}	—	—	—	—	260	256	261	270
—	—	—	—	314	—	—	—	—
ν_{CH}	7a	a_1 ip	—	413 (412;413;412)[a]	417	417	416	417
ν_{ring}	16b oop	b_1 oop	—	— (464;461;462)	472	472	471	470
δ_{ring}	6b	b_2 ip	—	617 (617;617;615)	617	613	612	613
δ_{ring}	6a	a_1 ip	698	698 (698;698;697)	692	692	692	691
γ_{CH}	11 oop	b_1 oop	734	736 (736;734;737)	733	737	740	738
γ_{CH}	10a oop	a_1 oop	835	834 (834;836;836)	—	—	—	—
ν_{C-S-H}	—	—	916	916 (914;920;914)	934	933	931	930
γ_{CH}	5 oop	b_1 oop	—	988 (991;991;991)	—	—	—	—
ν_{ring}	12	a_1 ip	1000	1000 (1002;1000;1000)	997	997	997	997
δ_{CH}	18a	a_1 ip	1025	1024 (1026;1025;1024)	1021	1021	1020	1020
δ_{CH}	18b	b_2 ip	1071	(—;—;1070)	1073	1073	1070	1069
ν_{ring}	1	a_1 ip	1091	1091 (1091;1097;1092)	—	—	—	—
Comb. mode	—	—	1118	1118 (—;—;1116)	1110	1111	1110	1109
δ_{CH}	9b	b_2 ip	1156	1157 (1159;1154;1157)	1156	1154	1157	1156
δ_{CH}	9a	a_1 ip	1181	1181 (1182;1180;1180)	1178	1178	1177	1178
δ_{CH}	19b	b_2 ip	1441	—	1434	1432	1435	1434
δ_{CH}	19a	a_1 ip	1478	— (—;—;1481)	1471	1470	1470	1470
ν_{ring}	8a	a_1 ip	1582	1584 (1582;1582;1581)	1572	1573	1572	1571
—	—	—	—	—	—		—	—
ν_{S-H}	—	—	2569	2567 (2575;2566;2566)	—	—	—	—

δ = in-plane deformation, γ = out-of-plane deformation, ν = stretching, ν_s = symmetric stretching. β_{as} = rocking, γ_s = wagging, β_s = scissoring, # = Wilson mode number, all modes in-plane if not stated otherwise oop: out-of-plane. [a] Numbers in bracket refer to the assignments bei Varsanyi[69] (first value), Kohlrausch[67] (second value), and Scott *et al.*[68] (third value); #: Wilson mode number.

A striking difference between SER spectra obtained in acidic and neutral solution is the overall scattering intensity. The generally much larger one with the neutral solution indicates a larger coverage or a pH-dependent orientation of the scattering molecules; surface enhancement itself does not appear to be pH-dependent. The difference in intensities can be rationalized when considering the pH-dependent dissociation equilibrium of TP. In the almost neutral electrolyte solution a larger fraction of thiolate ions may be available for adsorption, and although the dominating driving force of adsorption is the gold–sulfur bond energy the electrostatic interaction in particular at electrode potentials positive to the potential of zero charge E_{pzc} ($-0.18 < E_{pzc vs.SHE} < 0.34$ V, *i.e.* $-0.893 < E_{pzc vs.MSE} < -0.313$ V, ref. 8) appears to assist in adsorption yielding a higher coverage. In acidic solution the protonated form prevails and is adsorbed as evidenced with the band of the C–S–H bending mode. The electrostatic driving force is thus not as effective in supporting high coverage. Assessment of the influence of the pH-value on the adsorbate orientation and consequently on scattered intensity is presently too speculative. The CVs (Fig. 1–3) do not provide quantitative information about degree of coverage or number of adsorbed species, thus they are not in contradiction to this explanation.

Acknowledgements

Financial support from the Fonds der Chemischen Industrie and the Deutsche Forschungsgemeinschaft and help in acquiring some spectra and CVs from Monique Helmert and Hamidreza Sardary are gratefully acknowledged.

References

1 V. M. Mirsky, *TRAC*, 2002, **21**, 439–450.
2 A. L. Eckermann, D. J. Feld, J. A. Shaw and T. J. Meade, *Coord. Chem. Rev.*, 2010, **254**, 1769–1802.
3 J. Zhang, A. C. Welinder, Q. Chi and J. Ulstrup, *Phys. Chem. Chem. Phys.*, 2011, **13**, 5526–5545.
4 V. S. Dilimon, S. Rajalingam, J. Delhalle and Z. Mekhalif, *Phys. Chem. Chem. Phys.*, 2013, **15**, 16648–16656.
5 T. Baunach, V. Ivanova, D. A. Scherson and D. M. Kolb, *Langmuir*, 2004, **20**, 2797–2802.
6 E. Blomgren, J. O'M Bockris and C. Jesch, *J. Phys. Chem.*, 1961, **65**, 2000–2010.
7 J. O'M Bockris and K. T. Jeng, *J. Electroanal. Chem.*, 1992, **330**, 541–581.
8 For an overview of methods and results see: R. Holze, in *Landolt-Börnstein: Numerical Data and Functional Relationships in Science and Technology, New Series, Group IV: Physical Chemistry, Volume 9: Electrochemistry, Subvolume A: Electrochemical Thermodynamics and Kinetics*, ed. W. Martienssen and M. D. Lechner, Springer-Verlag, Berlin, 2007.
9 A. Ulman, *Chem. Rev.*, 1996, **96**, 1533–1554.
10 C. A. Szafranski, W. Tanner, P. E. Laibinis and R. L. Garrell, *Langmuir*, 1998, **14**, 3570–3579.
11 For a recent overview see: G. McNay, D. Eustace, W. E. Smith, K. Faulds and D. Graham, *Appl. Spectrosc.*, 2011, **65**, 825–837.
12 K. Carron and L. G. Hurley, *J. Phys. Chem.*, 1991, **95**, 9979–9984.
13 S. J. Li, D. Y. Wu, X. Y. Xu and R. N. Gu, *J. Raman Spectrosc.*, 2007, **38**, 1436–1443.
14 S. K. Saikin, Y. Z. Chu, D. Rappoport, K. B. Crozier and A. Aspuru-Guzik, *J. Phys. Chem. Lett.*, 2010, **1**, 2740–2746.
15 H.-L. Wu, H.-R. Tsai, Y.-T. Hung, K.-U. Lao, C.-W. Liao, P.-J. Chung, J.-S. Huang, I.-C. Chen and M. H. Huang, *Inorg. Chem.*, 2011, **50**, 8106–8111.
16 X.-Y. Xu, S.-J. Li, D.-Y. Wu and R.-A. Gu, *Acta Chim. Sin.*, 2007, **65**, 1095–1100.
17 J. Nara, S. Higai, Y. Morikawa and T. Ohno, *J. Chem. Phys.*, 2004, **120**, 6705–6711.
18 S. M. Ansar, X. Li, S. Zou and D. Zhang, *J. Phys. Chem. Lett.*, 2012, **3**, 560–565.
19 H. Yang, N. Gozubenli, Y. Fang and P. Jiang, *Langmuir*, 2013, **29**, 7674–7681.
20 Y. Jiao, D. S. Koktysh, N. Phambu and S. M. Weiss, *Appl. Phys. Lett.*, 2010, **97**, 53125.
21 J. Fontana, J. Livenere, F. J. Bezares, J. D. Caldwell, R. Rendell and B. R. Ratna, *Appl. Phys. Lett.*, 2013, **102**, 201606.
22 T. T. Nhung, Y. Bu and S.-W. Lee, *J. Cryst. Growth*, 2013, **373**, 132–137.
23 W. Hüttner, K. Christou, A. Göhmann, V. Beushausen and H. Wackerbarth, *Microfluid. Nanofluid.*, 2012, **12**, 521–527.
24 M. Moskovits, *Phys. Chem. Chem. Phys.*, 2013, **15**, 5301–5311.
25 J. R. Lombardi and R. L. Birke, *J. Chem. Phys.*, 2012, **136**, 144704.
26 J. R. Lombardi and R. L. Birke, *J. Phys. Chem. C*, 2008, **112**, 5605–5617.
27 S. W. Joo, *Chem. Lett.*, 2004, **33**, 60–61.
28 H. Xu, C. H. Tseng, T. J. Vickers, C. K. Mann and J. B. Schlenoff, *Surf. Sci.*, 1994, **311**, L707–L711.
29 M. A. Mahmoud and M. A. El-Sayed, *Nano Lett.*, 2009, **9**, 3025–3031.
30 K. D. Alexander, M. J. Hampton, S. P. Zhang, A. Dhawan, H. X. Xu and R. Lopez, *J. Raman Spectrosc.*, 2009, **40**, 2171–2175.
31 C. E. Taylor, J. E. Pemberton, G. G. Goodman and M. H. Schoenfisch, *Appl. Spectrosc.*, 1999, **53**, 1212–1221.
32 R. Buividas, N. Fahim, J. Juodkazyte and S. Juodkazis, *Appl. Phys. A: Mater. Sci. Process.*, 2014, **114**, 169–175.
33 B. Ren, G. Picardi, B. Pettinger, R. Schuster and G. Ertl, *Angew. Chem., Int. Ed.*, 2005, **44**, 139–142.
34 J. M. Marr and Z. D. Schultz, *J. Phys. Chem. Lett.*, 2013, **4**, 3268–3272.
35 X. M. Fan, W. J. Zou, R. A. Gu and J. L. Yao, *Chem. J. Chin. Univ.*, 2008, **29**, 130–134.
36 M. Wang, J. L. Yao and R. A. Gu, *Chem. J. Chin. Univ.*, 2006, **27**, 1518–1521.
37 X. Li, M. Cao, H. Zhang, L. Zhou, S. Cheng, J.-L. Yao and L.-J. Fan, *J. Colloid Interface Sci.*, 2012, **382**, 28–35.
38 L. Ling, M. M. Xu, R. A. Gu and J. L. Yao, *Acta Chim. Sin.*, 2007, **65**, 779–784.
39 Y. Cui, B. Ren, J. L. Yao, R. A. Gu and Z. Q. Tian, *J. Phys. Chem. B*, 2006, **110**, 4002–4006.
40 C. C. Chang, H. L. Wu, C. H. Kuo and M. H. Huang, *Chem. Mater.*, 2008, **20**, 7570–7574.
41 M. A. Mahmoud, *Langmuir*, 2013, **29**, 6253–6261.
42 M. A. Mahmoud and M. A. El-Sayed, *J. Phys. Chem. B*, 2013, **117**, 4468–4477.
43 T. Bhuvana, G. V. P. Kumar, G. U. Kulkarni and C. Narayana, *J. Phys. Chem. C*, 2007, **111**, 6700–6705.
44 Y. N. Kim, S. H. Yoo and S. O. Cho, *J. Phys. Chem. C*, 2009, **113**, 618–623.
45 S. J. Li and R. A. Gu, *Acta Chim. Sin.*, 2004, **62**, 2118–2122.
46 M. Ge, F. Bao, J. L. Yao, R. Sun and R. A. Gu, *Acta Chim. Sin.*, 2009, **67**, 2285–2289.
47 Y.-T. Tao, C.-C. Wu, J.-Y. Eu, W.-L. Lin, K.-C. Wu and C.-H. Chen, *Langmuir*, 1997, **13**, 4018–4023.
48 H. Sellers, A. Ulman, Y. Shnidman and J. E. Eilers, *J. Am. Chem. Soc.*, 1993, **115**, 9389–9401.
49 M. Tachibana, K. Yoshizawa, A. Ogawa, H. Fujimoto and R. Hoffmann, *J. Phys. Chem. B*, 2002, **106**, 12727–12736.
50 E. Sabatani, J. Cohen-Boulakia, M. Bruening and I. Rubinstein, *Langmuir*, 1993, **9**, 2974–2981.
51 K. S. Shin, *J. Raman Spectrosc.*, 2008, **39**, 468–473.
52 M. Futamata, *J. Phys. Chem.*, 1995, **99**, 11901–11908.
53 H. M. Lee, M. S. Kim and K. Kim, *Vib. Spectrosc.*, 1994, **6**, 205–214.
54 C. J. Sandroff and D. R. Herschbach, *J. Phys. Chem.*, 1982, **86**, 3277–3279.
55 M. Takahashi, M. Fujita and M. Ito, *Surf. Sci.*, 1985, **158**, 307–313.
56 M. Takahashi and M. Ito, *Chem. Phys. Lett.*, 1984, **103**, 512–516.
57 M. Takahashi, M. Fujita and M. Ito, *Chem. Phys. Lett.*, 1984, **109**, 122–127.

58 T. H. Joo, K. Kim and M. S. Kim, *J. Raman Spectrosc.*, 1987, **18**, 57–60.
59 F. G. Will and H. J. Hess, *J. Electrochem. Soc.*, 1973, **120**, 1–11.
60 F. G. Will, *J. Electrochem. Soc.*, 1986, **133**, 454–455.
61 R. Holze, *Surf. Sci.*, 1988, **202**, L612–L620.
62 T. Sueoka, J. Inukai and M. Ito, *J. Electron Spectrosc. Relat. Phenom.*, 1993, **64–65**, 363–370.
63 N. Hassan and R. Holze, *Elektrokhimiya*, 2012, **48**, 442–453; N. Hassan and R. Holze, *Russ. J. Electrochem.*, 2012, **48**, 401–411.
64 M. Bron and R. Holze, *205th Electrochemical Society Meeting*, San Antonio, TX, USA, 2004, abstract # 867.
65 M. Bron and R. Holze, *J. Solid State Electrochem.*, submitted.
66 R. Holze, *J. Solid State Electrochem.*, 2013, **17**, 1869–1879.
67 K. W. F. Kohlrausch, *Ramanspektren*, Akademische Verlagsgesellschaft Becker & Erler Leipzig, 1943.
68 D. W. Scott, J. P. McCullough, W. N. Hubbard, J. F. Messerly, I. A. Hossenlopp, F. R. Frow and G. Waddington, *J. Am. Chem. Soc.*, 1956, **78**, 5463–5468.
69 G. Varsányi, *Assignments for Vibrational Spectra of Seven Hundred Benzene Derivatives*, Adam Hilger, London, 1974.
70 J. H. S. Green, *Spectrochim. Acta*, 1968, **24A**, 1627–1637.
71 A. Wokaun, J. P. Gordon and P. F. Liao, *Phys. Rev. Lett.*, 1982, **48**, 957–960.
72 F. R. Dollish, W. G. Fateley and F. F. Bentley, *Characteristic Raman Frequencies of Organic Compounds*, Wiley, New York, 1974.
73 R. Holze, *Surface and Interface Analysis: An Electrochemists Toolbox*, Springer-Verlag, Heidelberg, 2009.
74 S. W. Joo, S. W. Han and K. Kim, *J. Phys. Chem. B*, 2000, **104**, 6218–6224.
75 S. W. Joo, S. W. Han and K. Kim, *Appl. Spectrosc.*, 2000, **54**, 378–383.
76 H. Kang, J. Noh, E. O. Ganbold, D. Uuriintuya, M. S. Gong, J. J. Oh and S. W. Joo, *J. Colloid Interface Sci.*, 2009, **336**, 648–653.
77 R. G. Greenler, *J. Chem. Phys.*, 1966, **44**, 310–315.
78 M. Moskovits, D. P. DiLella and K. J. Maynard, *Langmuir*, 1988, **4**, 67–76.
79 M. Moskovits, *J. Chem. Phys.*, 1982, **77**, 4408–4416.
80 J. S. Suh and M. Moskovits, *J. Am. Chem. Soc.*, 1986, **108**, 4711–4718.
81 M. Moskovits and J. S. Suh, *J. Phys. Chem.*, 1984, **88**, 5526–5530.
82 R. A. Wolkow and M. Moskovits, *J. Chem. Phys.*, 1992, **96**, 3966–3980.
83 J. E. Pemberton, M. A. Bryant, R. L. Sobocinski and S. L. Joa, *The 1991 Pittsburgh Conference*, Chicago, Ill, USA, 1991, abstr. 748.
84 R. Holze, *Bull. Electrochem.*, 1994, **10**, 45–55.

